

Observing the Sunyaev-Zel’dovich Effect Closer to Home

James E. Taylor^{1*}, Kavilan Moodley^{1,2} & J.M. Diego¹

¹*Denys Wilkinson Building, 1 Keble Road, Oxford OX1 3RH, United Kingdom*

²*School of Mathematical & Statistical Sciences, University of Natal, Durban, 4041, South Africa*

19 November 2018

ABSTRACT

Hot gas trapped in a dark matter halo will produce a decrement in the surface brightness of the microwave background, the Sunyaev-Zel’dovich (SZ) effect. While massive clusters produce the strongest central SZ decrements, we point out that a local galaxy halo, specifically the halo of M31, may be one of the brightest *integrated* SZ sources in the sky. For various realistic gas distributions consistent with current X-ray limits, we show that the integrated SZ decrement from M31 will be comparable to decrements already detected in more distant sources, provided its halo contains an appreciable quantity of hot gas. A measurement of this decrement would provide direct information on the mass, spatial distribution and thermodynamic state of hot gas in a low-mass halo, and could place important constraints on current models of galaxy formation. Detecting such an extended ($\sim 10^\circ$), low-amplitude signal will be challenging, but should be possible with all-sky SZ maps from satellite missions such as the Wilkinson Microwave Anisotropy Probe or the Planck Surveyor.

Key words: galaxies: haloes — galaxies: intergalactic medium — galaxies: M31 — cosmic microwave background

1 INTRODUCTION

The mean baryonic density of the Universe is now fairly well determined from nucleosynthesis (e.g. Burles, Nollett, & Turner 2001), the temperature fluctuation power spectrum of the cosmic microwave background (CMB) (Spergel et al. 2003), models of the Lyman alpha forest at high redshift (e.g. Hui et al. 2002), and the hot gas fraction in clusters (e.g. Roussel, Sadat & Blanchard 2000), together with constraints on the total matter density and the Hubble parameter, to be $\Omega_b \simeq 0.044$. As discussed by Silk (2003), there is a net shortfall in the baryons observed at the present day: about 20% are visible in the form of stars and cluster gas (Fukugita, Hogan and Peebles 1998), 20 % are in the low-redshift Lyman- α forest (Penton, Shull, & Stocke 2000), and about half of the remainder are predicted by simulations of structure formation to be in a diffuse, warm intergalactic medium (Cen & Ostriker 1999; Davé et al. 2001), for which there is also increasing observational evidence (e.g. Mathur, Weinberg, & Chen 2003). The missing 30% of the baryons, by implication, must be in some other phase, at densities and temperatures that are very hard to detect. Several pieces of observational evidence, including the break in the X-ray luminosity-temperature (L_x - T_x) relation on the scale of groups (e.g. Helsdon & Ponman 2000; Xue & Wu 2000) and

spectroscopic signatures of strong winds in damped Lyman-break systems (Shapley et al. 2002) suggest that this baryon deficit is connected with galaxy formation, which may eject a substantial fraction of the baryons out of dark matter haloes and into the IGM. If it is indeed true that galaxies process and eject a large fraction of the baryons in their haloes, then this is an important feature of galaxy formation that should be confirmed by direct observations of the residual hot gas in galaxy haloes.

In principle, the gas content of a dark matter halo can be determined directly from its X-ray emission, but whereas galaxy clusters emit strongly in the X-ray, due to their large gas content and high virial temperature, typical galaxy haloes will be much fainter X-ray emitters. Furthermore, galaxies themselves contain bright X-ray point sources, making emission from an extended, gaseous component around them harder to detect. Thus, while the non-detection of X-ray emission from a diffuse component in low-mass systems has set limits on the mass and mean density of gas surrounding typical galaxies (Benson et al. 2000), the constraints are relatively weak, and large quantities of low-density gas could easily be hiding in low-mass haloes.

The Sunyaev-Zel’dovich (SZ) effect, in which CMB photons are scattered to higher energies by collisions with hot electrons, provides a more sensitive way of detecting gas at low densities. This effect has now been measured with high signal-to-noise in many massive clusters (e.g. Ma-

* email: jet@astro.ox.ac.uk

son, Myers, & Readhead 2001; Grego et al. 2001; De Petris et al. 2002; see Rees et al. 2002 for earlier references), and increasing quantities of SZ data are becoming available from CMB experiments and dedicated instruments (see Carlstrom, Holder & Reese 2002 for a recent review). The central decrement produced by the SZ effect is independent of redshift, and varies in amplitude roughly as M , the mass of the cluster, so current SZ surveys generally focus on detecting the most massive galaxy clusters, irrespective of distance. The total SZ flux scattered by a source scales as $M^{5/3} d_a^{-2}$, however, where d_a is the angular diameter distance to the source. For a sufficiently nearby source, the larger apparent diameter can compensate for the mass dependence, making the gas in low-mass systems easier to detect.

In this letter, we suggest that one of the strongest integrated SZ signals may come from a galaxy halo, specifically the halo of our immediate neighbour M31. If this signal could be detected, it would offer a unique opportunity to study halo gas on a mass-scale that is very difficult to probe by other means. In what follows, we will first make a simple estimate of how the integrated (thermal) SZ flux and X-ray luminosity scale with mass and distance to the source, and compare the total signal from various nearby haloes. We will then calculate more precise values for M31, using a realistic model for the halo gas distribution. Finally, we will discuss the possibility of detecting a very low-amplitude temperature decrement from such an extended source, using data from all-sky CMB missions such as the Wilkinson Microwave Anisotropy Probe (WMAP) or the Planck Surveyor.

2 THE SZ FLUX FROM NEARBY HALOES

2.1 Basic Scaling

The thermal SZ effect is the temperature decrement produced when CMB photons are inverse-Compton scattered off hot gas along the line of sight. The relative decrement is proportional to the integral of the gas pressure, $P_e = n_e T_e$, along the line of sight. The integrated SZ flux, that is the total flux scattered in our direction by gas in a particular halo, is:

$$S(\nu)_{\text{SZ}} \propto g(\nu) I_o(\nu) \int d\Omega \int_0^{r_{\text{vir}}} n_e(\mathbf{r}) T_e(\mathbf{r}) dl \quad (1)$$

where the function $g(\nu)$ describes the frequency dependence of the SZ effect, $I_o(\nu)$ is the intensity of the CMB, $d\Omega$ is the solid angle subtended by the gas, r_{vir} is the virial radius of the halo, θ is the angle between the halo centre and the line of sight, and $l = (|r|^2 - \theta^2 d_a^2)^{1/2}$.

We can get a rough estimate of the magnitude of the SZ flux by assuming that the gas is isothermal, and that its temperature T_e is proportional to the virial temperature, $T_{\text{vir}} \propto M^{2/3}$. Integrating out to the virial radius $r_{\text{vir}} \propto M^{1/3}$, we then obtain the scaling relation $S(\nu)_{\text{SZ}} \propto M^{5/3} d_a^{-2}(z)$, where $d_a(z)$ is the (angular diameter) distance to the source.

Fig. 1 shows the estimated mass of various haloes, versus their estimated distance from us. The small black triangles are nearby groups or clusters from the UZC-SSRS2 catalogue (Ramella et al. 2002), with estimated distances derived from the redshift assuming zero peculiar velocity, and

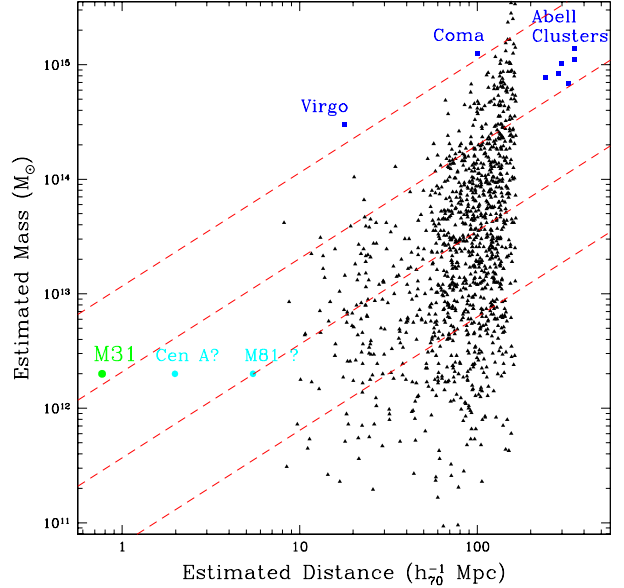


Figure 1. Estimated (angular diameter) distances and masses for nearby galaxy, group and cluster haloes. The small triangles are from the UZC-SSRS2 catalogue (Ramella et al. 2002) of nearby groups and clusters, while the large points show the loci of specific objects with distances and halo masses estimated by various means (see text for details). Lines indicate constant integrated SZ flux, assuming a simple scaling with mass and distance.

estimated masses as given in the catalogue. We also include various nearby galaxy and cluster haloes (large points), with their names indicated. The distances and masses for these objects were taken from the Lyon-Meudon Extragalactic Database (LEDA) and from various recent references (Virgo – Schindler, Binggeli, & Böhringer 1999; Fouqué et al. 2001; Coma – Liu & Graham 2001). For M81 and Cen A, we assumed the same halo mass as M31. The more distant points are a set of Abell clusters for which the SZ effect has been measured (Mason et al. 2001), with distances based on their redshift and masses scaled up from the mass of Coma by $(T_{\text{Abell}}/T_{\text{Coma}})^{3/2}$. We assume a Hubble constant of $70 \text{ km s}^{-1} \text{ Mpc}^{-1}$ in all cases.

Both the mass and the distance estimates plotted here contain substantial uncertainties. Nonetheless, they give a general indication of representative values for nearby haloes. Also indicated on the plot are lines of constant integrated SZ flux, assuming the scaling $S(\nu)_{\text{SZ}} \propto M^{5/3} d_a^{-2}$. We see that Coma stands out as one of the most massive nearby clusters; indeed, it was recently detected at about the $10\text{-}\sigma$ level (that is 5 , 0.5 and $5\text{-}\sigma$ in 3 separate bands) by De Petris et al. (2002), for instance. We also see that there are various other promising targets for SZ observations, including Virgo and the Abell clusters. At very small distances, however, another source stands out: the halo of M31. Although a thousand times less massive than the Abell clusters, it is close enough that it may produce a comparable SZ flux locally.

An extended halo around M31 might also be detectable in X-rays. We can estimate the X-ray luminosity from gas in the halo of M31, for the simple isothermal gas distribution considered above. The total X-ray luminosity is:

$$L_X = \int dV n_e^2 \Lambda(T) dr. \quad (2)$$

Here $\Lambda(T)$ is the X-ray emissivity, which consists of a bremsstrahlung term scaling as $T^{1/2}$, and a term due to spectral lines. For simplicity, we will assume the line emission has the same scaling with T , and increases the total luminosity by a factor of roughly 2 (as appropriate for a low metallicity gas in the 0.5–2.0 keV band). The total luminosity should therefore scale as $L_x \propto M n_e(0)^2 T^{1/2} \propto M^{4/3} n_e(0)^2$. Thus, even a massive halo of gas may escape detection provided it is sufficiently extended, so that n_e is low.

In fact, recent ASCA observations by Takahashi et al. (2001) place an upper limit of $2.3 \pm 0.3 \times 10^{38} \text{ erg s}^{-1}$ on soft (0.5–10 keV) emission from within 12' (or 2.7 kpc at a distance of 770 kpc) of the centre of M31, while an earlier analysis of ROSAT data by West, Barber and Folgheraiter (1997) limited the contribution to the luminosity from within 21.5 kpc (at 770 kpc) to less than $5.4 \times 10^{39} \text{ erg s}^{-1}$ in the 0.5–2.0 keV band, assuming M31 has the same mass as the Milky Way. We will scale this mass up to $10^{40} \text{ erg s}^{-1}$, on the assumption that M31 is at least 50 per cent more massive than the Milky Way, as implied by its greater circular velocity. As we will show below, these limits do not constrain the mass of gas in the halo of M31 very strongly, provided the gas is distributed well beyond the optical extent of the galaxy.

So far in this discussion we have assumed simple scalings for the sizes, temperatures and densities of halo gas distributions. Observations show that real systems deviate from these simple assumptions. The relationship between X-ray luminosity and temperature is a power-law for massive clusters, for instance, but changes slope on group and galaxy scales (e.g. Helsdon & Ponman 2000; Xue & Wu 2000 and references therein). Overall, low-mass haloes are less X-ray luminous than expected from simple scalings or from galaxy formation models (Benson et al. 2000). This could indicate that low-mass haloes contain little hot gas, their primordial gas having cooled and/or having been ejected at some point in the halo's history. In this case, the SZ effect may be undetectable on galaxy scales. Alternatively, however, the gas may be present in an extended, low-density distribution. In this case, the X-ray signal will be reduced, but the total SZ flux will be unaffected. We investigate these possibilities in more detail below.

2.2 Simple Halo Models

We will now consider more detailed models of the gas distribution in the halo of M31, to calculate realistic values for the total SZ decrement and X-ray luminosity. The distribution of hot gas in galaxy clusters is reasonably well described by an empirically-derived fitting function, the beta profile,

$$n_e(r) = n_e(0)(1 + (r/r_c)^2)^{-3\beta/2} \quad (3)$$

(Cavaliere & Fusco-Femiano 1978). We will assume $\beta = 2/3$, since this is the value which best matches cluster X-ray profiles (Jones & Foreman 1984; Mohr, Mathiesen, & Evrard 1999). For this particular model, if the gas is isothermal, then the integrated SZ flux from within a projected radius R is:

$$S_{\text{SZ}}(R, \nu) = S_0 g(\nu) \left(\frac{n_e(0)}{10^{-3} \text{cm}^{-3}} \right) \left(\frac{T_e}{1 \text{keV}} \right) \left(\frac{r_c}{1 \text{kpc}} \right)^3 f_1(R), \quad (4)$$

where $S_0 = 3.615 \times 10^{-3} \text{ Jy}$ (assuming a distance of 770 kpc to M31), $g(\nu)$ is a function of order 1 describing the frequency dependence of the effect, and $f_1(R) = [(1 + (R/r_c)^2)^{1/2} - 1]$. The contribution to the bolometric X-ray luminosity from within the same radius is:

$$L_X(R) = L_{X,0} \left(\frac{n_e(0)}{10^{-3} \text{cm}^{-3}} \right)^2 \left(\frac{T}{1 \text{keV}} \right)^{0.5} \left(\frac{r_c}{1 \text{kpc}} \right)^3 f_2(R), \quad (5)$$

where $L_{X,0} = 1.10 \times 10^{35} \text{ erg s}^{-1}$ (assuming the dominant contribution is from free-free emission, and that line emission is negligible) and $f_2(R) = [1 - (1 + (R/r_c)^2)^{-1/2}]$. The electron density is normalised by specifying the mass within some radius $M_{\text{hot}}(< R) = 4\pi m_p \mu n_e(0) r_c^{-3} [(R/r_c) - \tan^{-1}(R/r_c)]$. We note that the gas distribution in simulated haloes drops off faster than r^{-2} in the outer parts, so if we integrated the beta profile out to the virial radius of the halo we would overestimate the mass in the outer regions. To avoid this complication, we consider only the mass within the central 100 kpc of the halo, and use this to set $n_e(0)$.

To determine the amplitude of the SZ and X-ray emission, we need to fix the values of T , $M_{\text{hot}}(< 100 \text{ kpc})$, and r_c . We will assume that the gas in the halo of M31 follows the mass-temperature relation observed for slightly more massive group haloes, so that $T \simeq 0.5 \text{ keV}$. For $M_{\text{hot}}(< 100 \text{ kpc})$, the total mass of hot gas within the central 100 kpc, we have the constraint that the baryon fraction of the whole halo not exceed the universal value $f_b = \Omega_b/\Omega_m = 0.166$ (Spergel et al. 2003). The mass of the halo of M31 is estimated to be between 1 and $2 \times 10^{12} M_\odot$ (Klypin, Zhao, & Somerville 2002). Thus its total, primordial baryonic mass would have been $1.66 - 3.32 \times 10^{11} M_\odot$, of which approximately $9 \times 10^{10} M_\odot$ are in the form of stars and gas in the galaxy itself. This leaves up to $\simeq 2.4 \times 10^{11} M_\odot$ of hot gas in the halo. If this gas traced the dark matter distribution, roughly half of it would lie in the central 100 kpc of the system (assuming a virial radius of 330 kpc). Then again, radiative cooling or galactic heating may have altered the gas distribution, causing it to be more or less centrally condensed. We will consider values of M_{hot} between 10^{10} and $1.5 \times 10^{11} M_\odot$, which should cover a realistic range in mass.

Finally, we have to choose a value for the core radius of the gas distribution, r_c . Detailed models of cluster gas suggest that this should be roughly equal to the core radius of the dark matter distribution, $r_{c,\text{DM}}$, which is 27.5 kpc for a halo mass of $2 \times 10^{12} M_\odot$ in a LCDM cosmology (Eke, Navarro & Steinmetz 2001). On the other hand, there has been recent observational evidence for a much larger, lower density distribution of gas around the Milky Way, extending out to 70 kpc or more (Sembach et al. 2002). Given this uncertainty, for each model we will choose the smallest core radius consistent with the X-ray limits discussed previously, which will generally be larger than $r_{c,\text{DM}}$. Slightly larger or smaller core radii will have little effect on the detectability of the SZ signal, which depends mainly on M_{hot} , as shown below.

Table 1. Model Gas Distributions

Model	M_{hot} ($10^{11} M_{\odot}$)	r_c (kpc)	r_c ($^{\circ}$)	$L_X(< r_1)$ ($10^{38} \text{ erg s}^{-1}$)	$L_X(< r_2)$ ($10^{38} \text{ erg s}^{-1}$)	$S_{\text{SZ}}(< r_c)$ (Jy @ 150 GHz)	$S_{\text{SZ}}(< 100 \text{ kpc})$ (Jy @ 150 GHz)
A	1.5	57	4.2	1.6	94	-11.3	-27.8
B	1.0	48	3.6	1.7	95	-7.5	-23.8
C	0.5	36	2.7	1.8	91	-3.8	-17.7
D	0.3	29	2.2	1.9	87	-2.3	-14.1
E	0.2	24	1.8	2.2	89	-1.5	-11.9
F	0.1	18	1.3	2.3	74	-0.8	-8.4

In table 1 we give the SZ and X-ray emission from various model haloes, with parameters chosen based on these arguments. We calculate the integrated SZ flux from within the core radius and 100 kpc, as well as the X-ray luminosity from the two regions for which there are observational limits, $r_1 = 2.7$ kpc and $r_2 = 21.5$ kpc. We see that the SZ flux from some models can be very large, while the total X-ray luminosity is still below the observational limits. To determine whether any of these gas distributions would be detected, however, we have to estimate the noise level in SZ maps filtered on large scales. We will make a rough calculation of the signal-to-noise in the next section. First, however, we consider the additional contribution to the signal from the kinetic SZ effect.

2.3 Kinetic SZ effect

Motion of gas with respect to the CMB also produces a second, kinetic SZ effect with a distinct spectral signature. The amplitude of the kinetic effect relative to the thermal effect is:

$$S_0^k/S_0^t(\nu) = \left(\frac{1.67}{j(\nu)} \right) \left(\frac{v_{\text{CMB}}}{1000 \text{ km s}^{-1}} \right) \left(\frac{T_e}{1.0 \text{ keV}} \right)^{-1}, \quad (6)$$

where $j(\nu)$ is a function of order one describing the spectral dependence and v_{CMB} is the velocity of the gas with respect to the CMB. For clusters, where T_e is large, this ratio is typically less than 10 per cent, but in M31 T_e would be much lower, and thus the kinetic effect could boost the SZ signal substantially. If we assume the gas is moving with the same velocity as the central galaxy (whose motion is almost opposite to the CMB dipole), then $v_{\text{CMB}} = 582 \text{ km s}^{-1}$, and at 150 GHz, $S_0^k/S_0^t \simeq 2$, so the combined SZ flux will be three times larger at this frequency. The halo of M31 may also rotate at an appreciable velocity, of course, which would modulate this contribution. Finally, we note that the thermal and kinetic contributions to this signal can in principle be separated, due to their different frequency dependence. Thus it could provide the first strong detection of the kinetic SZ effect. This separation will require good spatial resolution and excellent signal-to-noise, however, since the frequency dependence of the kinetic SZ signal is the same as that of the CMB.

2.4 Detection Strategies

For the models considered above, we expect a total SZ flux of $\simeq 1$ –10 Janskys or more, spread out over a patch several degrees in size. While this signal is comparable to those

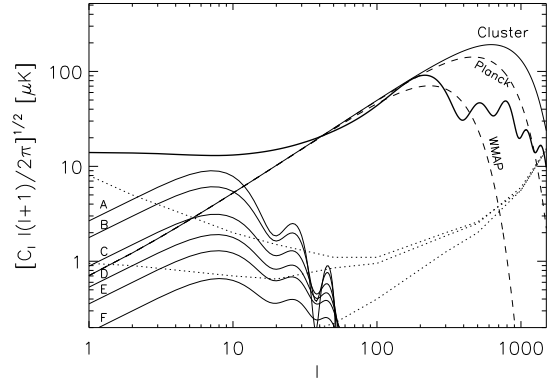


Figure 2. The angular power spectrum (RJ) for the models listed in table 1 (thin solid curves), compared with the power spectrum of primordial anisotropies (thick curve), and various estimates of the (RJ) residuals in Planck maps (dotted lines; Tegmark et al. 2000). Also shown is the power spectrum for a typical Abell cluster, and the same spectrum convolved with the WMAP and Planck beams (dashed curves).

detected from much more compact sources such as distant clusters, it may be harder to extract from SZ maps contaminated by residuals from primary anisotropies or large-scale foregrounds. We have estimated the contribution of our models to the power spectrum of the Rayleigh-Jeans (RJ) regime in the Planck maps. Since the power spectrum is an average quantity over the sky, our estimates need to be re-scaled by an area correction factor in order to make a fair comparison. In Fig. 2, we compare the contribution from the models to estimates of the residuals in Planck SZ maps (Tegmark et al. 2000), making pessimistic, realistic, or optimistic assumptions about the efficiency of foreground subtraction (dotted lines, from top to bottom). We see that for realistic assumptions about foreground subtraction (middle dotted line), our models are detectable at the 1–10 σ level on 20 $^{\circ}$ scales. The kinetic contribution could increase the signal by an additional factor of 2–3, provided it could be separated from the CMB itself.

We note that M31 lies in a zone of reasonably low foregrounds. Fig. 3 shows a section of the SFD dust map (Schlegel, Finkbeiner, & Davis 1998) centred on M31. The circle indicates a projected radius of 7.4 $^{\circ}$, or 100 kpc at a distance of 770 kpc. Since we know the centre of the halo gas distribution a priori, we may be able to optimise the SZ detection further, by using filters centred on this point or focusing on the parts of this region less contaminated by

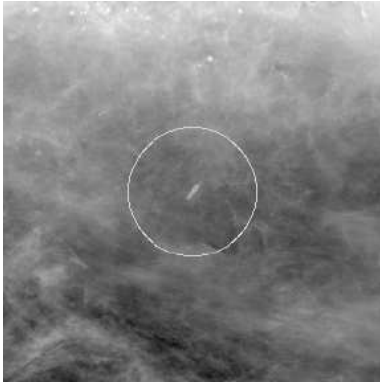


Figure 3. A section of the SFD dust map (Schlegel et al. 1998), centred on M31. The patch within 100 kpc of the galaxy (indicated by the circle) is relatively free of foreground dust emission.

foregrounds. Given the low amplitude and large spatial extent of the source, the signal from M31 will probably not be detectable by interferometers. The data from the WMAP mission is more promising in this regard, although it is also at lower frequency where the relative contribution from the thermal SZ effect is smaller. Recent analysis by Tegmark, de Oliveira-Costa & Hamilton (2003) finds that WMAP residuals have an r.m.s. amplitude of $4\text{--}5 \mu\text{K}$ at $l = 10$ in the cleanest regions of the sky. Using a naive combination of WMAP frequencies (Q-W bands) to subtract the CMB, we expect roughly 6 times less signal from the SZ effect than in the RJ regime assumed in Fig. 2, so even model ‘A’ would not be detectable above this noise level without using more elaborate methods. On the other hand, the 4-year WMAP data may start to rule out the most massive of our halo models.

3 DISCUSSION

We have shown that for a series of realistic models, the halo of M31 should produce a substantial integrated SZ flux. While the precise extent and amplitude of the flux depend on the details of the gas distribution, more elaborate models should produce roughly the same values as calculated here. In particular, since the SZ effect depends on the integral of the electron pressure along the line of sight, we expect the same total flux even if the pressure support for the halo gas close to M31 itself comes from a hotter, lower-density component heated by galactic sources, as suggested by X-ray observations (e.g. Takahashi et al. 2001).

From the calculations above, the integrated SZ flux should be detectable at the $1\text{--}10\sigma$ level in SZ maps based on Planck data, provided that the foreground removal is reasonably accurate, and that the halo of M31 still contains a reasonable amount of hot gas. If this signal is detected, it will provide a direct determination of the thermodynamic properties of halo gas on galaxy scales. Conversely, if the SZ effect is not detected it will place useful constraints on the amount of gas left over after the formation of a spiral galaxy within this halo. We do not expect the SZ signal from M31 to be visible in the first-year WMAP data, but the 4-year data should also start to constrain the gas distribution in its halo. Thus CMB experiments may soon provide an

unexpected view of the effects of galaxy formation close at hand.

ACKNOWLEDGEMENTS

The authors would like to thank Nabila Aghanim, Greg Bryan, Marc Sarzi and Joe Silk for useful discussions. JET acknowledges support from the Leverhulme Trust during the course of this work. KM acknowledges the support of a PPARC Fellowship (PPA/G/S/1999/00671). JMD acknowledges the support of a Marie Curie Fellowship from the European Community (HPMF-CT-200-00967). The dust map shown in Fig. 3 was generated using NASA’s SkyView facility, located at NASA Goddard Space Flight Center (<http://skyview.gsfc.nasa.gov>).

REFERENCES

- Benson, A. J., Bower, R. G., Frenk, C. S., & White, S. D. M. 2000, *MNRAS*, 314, 557
- Burles, S., Nollett, K. M., & Turner, M. S. 2001, *ApJL*, 552, L1
- Carlstrom, J. E., Holder, G. P., & Reese, E. D. 2002, *ARAA*, 40, 643
- Cavaliere, A. & Fusco-Femiano, R. 1978, *AAp*, 70, 677
- Cen, R. & Ostriker, J. P. 1999, *ApJ*, 514, 1
- Davé, R. et al. 2001, *ApJ*, 552, 473
- De Petris, M. et al. 2002, *ApJL*, 574, L119
- Eke, V. R., Navarro, J. F., & Steinmetz, M. 2001, *ApJ*, 554, 114
- Fouqué, P., Solanes, J. M., Sanchis, T., & Balkowski, C. 2001, *AAp*, 375, 770
- Fukugita, M., Hogan, C. J., & Peebles, P. J. E. 1998, *ApJ*, 503, 518
- Grego, L., Carlstrom, J. E., Reese, E. D., Holder, G. P., Holzappel, W. L., Joy, M. K., Mohr, J. J., & Patel, S. 2001, *ApJ*, 552, 2
- Helsdon, S. F. & Ponman, T. J. 2000, *MNRAS*, 315, 356
- Hui, L., Haiman, Z., Zalduendo, M., & Alexander, T. 2002, *ApJ*, 564, 525
- Jones, C. & Forman, W. 1984, *ApJ*, 276, 38
- Klypin, A., Zhao, H., & Somerville, R. S. 2002, *ApJ*, 573, 597
- Liu, M. C. & Graham, J. R. 2001, *ApJL*, 557, L31
- Mason, B. S., Myers, S. T., & Readhead, A. C. S. 2001, *ApJL*, 555, L11
- Mathur, S., Weinberg, D. H., & Chen, X. 2003, *ApJ*, 582, 82
- Mohr, J. J., Mathiesen, B., & Evrard, A. E. 1999, *ApJ*, 517, 627
- Penton, S. V., Shull, J. M., & Stocke, J. T. 2000, *ApJ*, 544, 150
- Ramella, M., Geller, M. J., Pisani, A., & da Costa, L. N. 2002, *AJ*, 123, 2976
- Reese, E. D., Carlstrom, J. E., Joy, M., Mohr, J. J., Grego, L., & Holzappel, W. L. 2002, *ApJ*, 581, 53
- Roussel, H., Sadat, R., & Blanchard, A. 2000, *AAp*, 361, 429
- Schindler, S., Binggeli, B., & Böhringer, H. 1999, *AAp*, 343, 420
- Schlegel, D. J., Finkbeiner, D. P., & Davis, M. 1998, *ApJ*, 500, 525
- Sembach, K. R., et al. 2002, *ApJ*, submitted (astro-ph/0207562)
- Shapley, A., Steidel, C., Adelberger, K., & Pettini, M. 2002, in ‘A New Era in Cosmology’, T. Shanks & N. Metcalf eds., in press (astro-ph/0107324)
- Silk, J., 2003, *MNRAS*, submitted (astro-ph/0212068)
- Spergel, D. N., et al. 2003, *ApJ* submitted (astro-ph/0302209)
- Takahashi, H., Okada, Y., Kokubun, M., & Makishima, K. 2001, *PASJ*, 53, 875
- Tegmark, M., Eisenstein, D. J., Hu, W., & de Oliveira-Costa, A. 2000, *ApJ*, 530, 133
- Tegmark, M., de Oliveira-Costa, A., & Hamilton, A. J. S. 2003, *PRD*, submitted (astro-ph/0302496)
- West, R. G., Barber, C. R., & Folgheraiter, E. L. 1997, *MNRAS*, 287, 10
- Xue, Y. & Wu, X. 2000, *ApJ*, 538, 65